Nuclear Engineering and Technology 52 (2020) 2522–2534

Contents lists available at ScienceDirect

Nuclear Engineering and Technology

journal homepage: www.elsevier.com/locate/net

Original Article

Disturbance observer based adaptive sliding mode control for power tracking of PWRs

Jiuwu Hui, Jingqi Yuan*

Department of Automation, the Key Laboratory of System Control and Information Processing/Ministry of Education, Shanghai Jiao Tong University, 800 Dongchuan Road, 200240, Shanghai, China

ARTICLE INFO

Article history:
Received 21 January 2020
Received in revised form
25 April 2020
Accepted 27 April 2020
Available online 23 May 2020

Keywords:
Pressurized-water reactor (PWR)
Power tracking
Point-reactor kinetics equations
Disturbance observer (DOB)
Adaptive sliding mode control (ASMC)

ABSTRACT

It is well known that the model of nuclear reactors features natural nonlinearity, and variable parameters during power tracking operation. In this paper, a disturbance observer-based adaptive sliding mode control (DOB-ASMC) strategy is proposed for power tracking of the pressurized-water reactor (PWR) in the presence of lumped disturbances. The nuclear reactor model is firstly established based on point-reactor kinetics equations with six delayed neutron groups. Then, a new sliding mode disturbance observer is designed to estimate the lumped disturbance, and its stability is discussed. On the basis of the developed DOB, an adaptive sliding mode control scheme is proposed, which is a combination of backstepping technique and integral sliding mode control approach. In addition, an adaptive law is introduced to enhance the robustness of a PWR with disturbances. The asymptotic stability of the overall control system is verified by Lyapunov stability theory. Simulation results are provided to demonstrate that the proposed DOB-ASMC strategy has better power tracking performance than conventional sliding mode controller and PID control method as well as conventional backstepping controller.

1. Introduction

Nowadays, nuclear energy has become one of the most mature, secure, economic, sanitary, potential and promising new energy source. Due to serious energy crisis in the world, construction of nuclear power plants has been significantly important in the development of international economy. In spite of the accidents at Chernobyl and Fukushima nuclear power plants, construction of nuclear power plants in the world is still developing steadily [1].

Power tracking problem of a nuclear power plant is a bigger challenge because of the characteristics of the nuclear reactor model, such as natural nonlinearity and multiple uncertainties due to random external disturbances and parameter variations. In the literature, researchers have proposed various kinds of control schemes to improve on power tracking performance, such as multivariable PI control [2], optimized PID control [3], fuzzy control [4,5], model predictive control [6,7], disturbance rejection control [8], sliding mode control (SMC) [9–12], and adaptive robustness control [13,14]. It is worthwhile to mention that SMC is a popular and effective control approach, and it features strong robustness with respect to external disturbances and insensitivity to parameter uncertainties [15]. In addition, SMC is widely used in control system of the nuclear power plant, such as water-level control of nuclear steam generators [16], turbine throttle pressure regulation [17], and power-level control [9,11,12]. In Ref. [9], a nonlinear adaptive sliding mode control approach is developed based on Takagi-Sugeno fuzzy models for modular high-temperature gas-cooled reactors, and simulations are presented by the comparisons between the developed control approach and conventional nonlinear sliding mode control as well as PID control. In Ref. [11], a reduced-order fractional-order sliding mode controller is designed to track the reference power trajectory for a nuclear power plant and deal with model uncertainties and external disturbances simultaneously. Reddy et al. [12] proposed a robust sliding mode control scheme using a new computationally efficient formulation of the multirate output feedback for spatial power control of a pressurized heavy water reactor (PHWR) with disturbances. Moreover, in this work, xenon and iodine dynamics are considered in the nonlinear model of a PHWR.

Those aforementioned control strategies provide an effective way to track desired power and robustly deal with model uncertainties and external disturbances in some specific cases, which implies that the disturbances rejection ability is improved at the

* Corresponding author.
E-mail addresses: huijiuwu@sjtu.edu.cn (J. Hui), jqyuan@sjtu.edu.cn (J. Yuan).

https://doi.org/10.1016/j.net.2020.04.027
1738-5733/

price of sacrificing the nominal power tracking performance. In recent years, in order to handle disturbances and maintain nominal control performance simultaneously, the disturbance observer (DOB) is widely introduced into advanced control approaches by researchers. For instance, Chen and Yu [18] combined a sliding mode disturbance observer with SMC for attitude tracking of near-space vehicles. Liu et al. [19] developed a nonlinear disturbance observer based nonlinear model predictive control strategy to deal with autonomous flight problem for small helicopters. The designed nonlinear DOB is applied to estimate external force/torque caused by wind turbulences, unmodeled dynamics and variations of the helicopter dynamics. Yang et al. [20] presented a decentralized adaptive robust controller for trajectory tracking of robot manipulators. A DOB is introduced to compensate for the low-passed coupled uncertainties.

Inspired by all the above analysis, a disturbance observer-based adaptive sliding mode control (DOB-ASMC) strategy is proposed to address the problem of power tracking of a pressurized-water reactor (PWR) with disturbances. The mathematical model of the PWR is firstly described based on point-reactor kinetics equations. Subsequently, a new sliding mode disturbance observer is developed to estimate the lumped disturbances including reactivity disturbances, model uncertainties, and external disturbances. Making use of the estimation values of disturbances from the DOB, an adaptive sliding mode control approach is proposed based on the combination of backstepping technique and integral sliding mode control method. The stability of the overall closed-loop system is investigated according to the Lyapunov stability theory. At last, simulation studies show that the proposed DOB-ASMC strategy has better power tracking performance compared to the conventional SMC scheme and PID power controller as well as conventional backstepping controller, namely, higher tracking accuracy, better disturbance rejection capability, and stronger robustness with respect to disturbances.

The rest of this paper is organized as follows. In Section 2, the mathematical model of the PWR is firstly described based on point-reactor kinetics equations. In Section 3, a new sliding mode disturbance observer is developed to estimate the lumped disturbances. The systematic design procedure of the DOB-ASMC strategy is presented in Section 4. Simulation results are provided in Section 5. Section 6 concludes this paper.

2. Mathematical model of the PWR

Here the mathematical model of the PWR is established including point-reactor kinetics equations with six delayed neutron groups, reactivity equations, and fuel and coolant thermal-hydraulics equations. Those aforementioned equations are described with respect to nominal equilibrium condition. In addition, it is worthwhile pointing out that point-reactor kinetics equations are applicable to near nominal equilibrium condition [21,22] and have been widely applied in power tracking study for nuclear power plants [23–25]. The point-reactor kinetics equations are given as

$$\frac{\mathrm{d}n_r}{\mathrm{d}t}=\frac{\rho-\beta}{\Lambda}n_r+\sum_{i=1}^{6}\frac{\beta_i}{\Lambda}c_{ri}+d \quad (1)$$

$$\frac{\mathrm{d}c_{ri}}{\mathrm{d}t}=\lambda_i n_r-\lambda_i c_{ri} \quad (2)$$

where n_r, c_{ri}, Λ, λ_i, ρ, β_i and d denote relative neutron density, relative density of ith delayed neutron precursor, neutron generation time, decay constant of ith delayed neutron precursor, total reactivity, ith delayed neutron fraction, and lumped disturbances due to model uncertainties and external disturbances, respectively.

Table 1
Parameter values of the PWR model.

Parameter	Value	Unit
P_0	900	MW
β_1	0.000247	–
β_2	0.001385	–
β_3	0.001222	–
β_4	0.002645	–
β_5	0.0008325	–
β_6	0.000169	–
λ_1	0.0124	s^{-1}
λ_2	0.0305	s^{-1}
λ_3	0.111	s^{-1}
λ_4	0.301	s^{-1}
λ_5	1.14	s^{-1}
λ_6	3.01	s^{-1}
Λ	0.08	S
f_f	0.92	–
Ω	6.6	MW/°C
μ_c	71.8	MW.s/°C
μ_f	26.3	MW.s/°C
α_f	-3.24×10^{-5}	$^{\circ}C^{-1}$
α_c	-2.13×10^{-4}	$^{\circ}C^{-1}$
G_r	0.02	m^{-1}

Assuming that there exist reactivity disturbances due to xenon oscillation, power defect, and fuel burnup etc. Meanwhile, taking into account the temperature effect of the fuel and coolant, the reactivity equations are given as

$$\rho=\rho_r+\alpha_f\left(T_f-T_{f0}\right)+\frac{\alpha_c}{2}\left(T_l-T_{l0}\right)+\frac{\alpha_c}{2}\left(T_e-T_{e0}\right)+\Delta_\rho \quad (3)$$

$$\frac{\mathrm{d}\rho_r}{\mathrm{d}t}=G_r Z_r+d_1 \quad (4)$$

where T_f, T_l, T_e, α_f, α_c, ρ_r, G_r, and Z_r denote average fuel temperature, temperature of the coolant leaving the reactor, temperature of the coolant entering the reactor, fuel temperature coefficient, coolant temperature coefficient, reactivity due to the position movement of control rod, reactivity worth and speed of control rod, respectively; T_{f0}, T_{l0} and T_{e0} represent initial average fuel temperature, temperature of the coolant leaving the reactor, and temperature of the coolant entering the reactor, respectively; Δ_ρ denote reactivity disturbances due to xenon oscillation, power defect, and fuel burnup etc., and d_1 denote input uncertainties.

The thermal-hydraulics equations of the fuel and coolant are described as

$$\frac{\mathrm{d}T_f}{\mathrm{d}t}=\frac{f_f P_0}{\mu_f}n_r-\frac{\Omega}{\mu_f}T_f+\frac{\Omega}{2\mu_f}T_l+\frac{\Omega}{2\mu_f}T_e \quad (5)$$

$$\frac{\mathrm{d}T_l}{\mathrm{d}t}=\frac{\left(1-f_f\right)P_0}{\mu_c}n_r+\frac{\Omega}{\mu_c}T_f-\frac{2M+\Omega}{2\mu_c}T_l+\frac{2M-\Omega}{2\mu_c}T_e \quad (6)$$

where μ_f, μ_c, M, Ω, f_f, and P_0 denote fuel total heat capacity, coolant total heat capacity, mass flow rate times heat capacity of the coolant, heat transfer coefficient between coolant and fuel, fraction of reactor power deposited in the fuel, and nominal power, respectively. The output power is given as

$$P(t)=P_0 n_r(t) \quad (7)$$

Substituting (3) into (1) yields

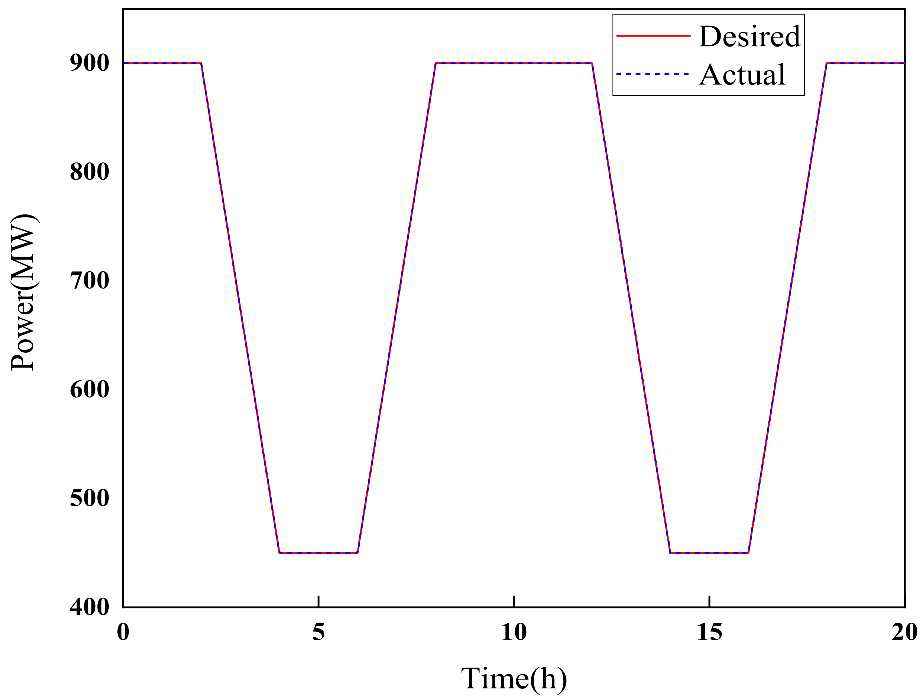

Fig. 1. Power tracking performance under the action of the DOB-ASMC scheme.

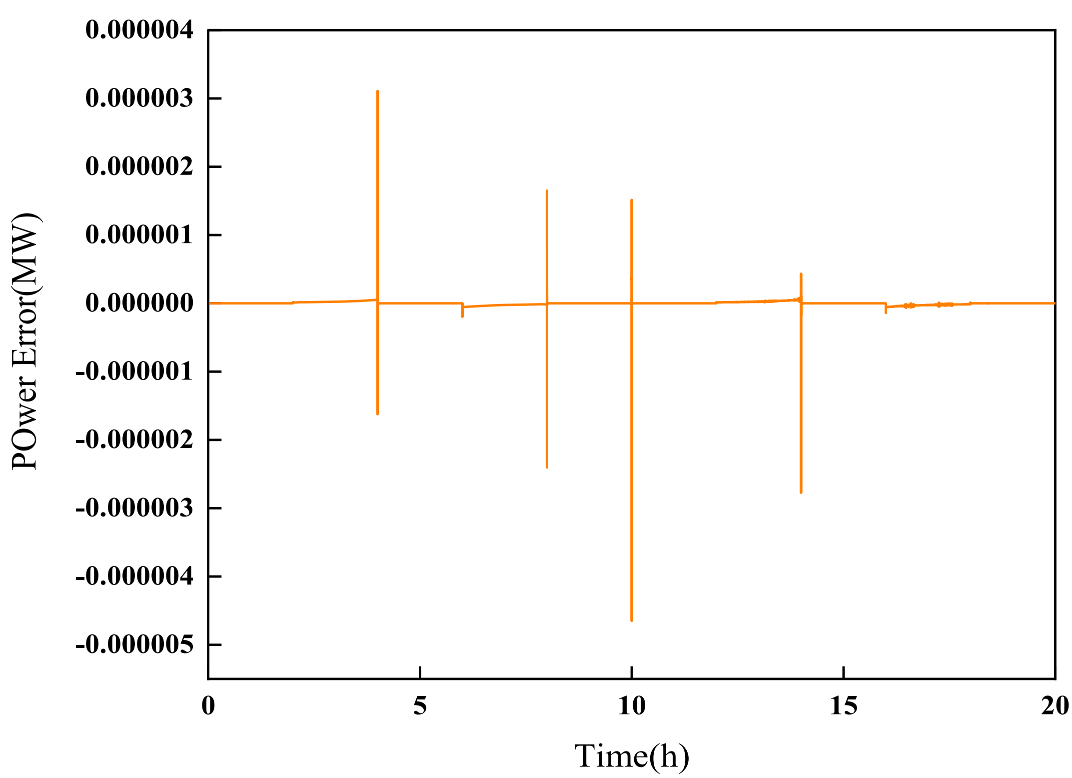

Fig. 2. Power tracking error under the action of the DOB-ASMC scheme.

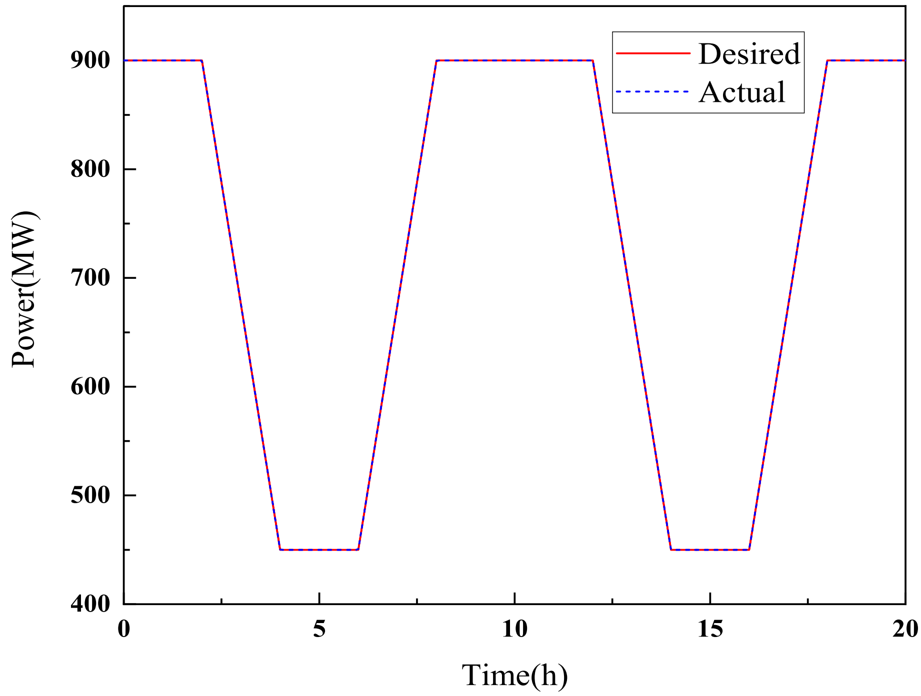

Fig. 3. Power tracking performance under the action of the conventional SMC scheme.

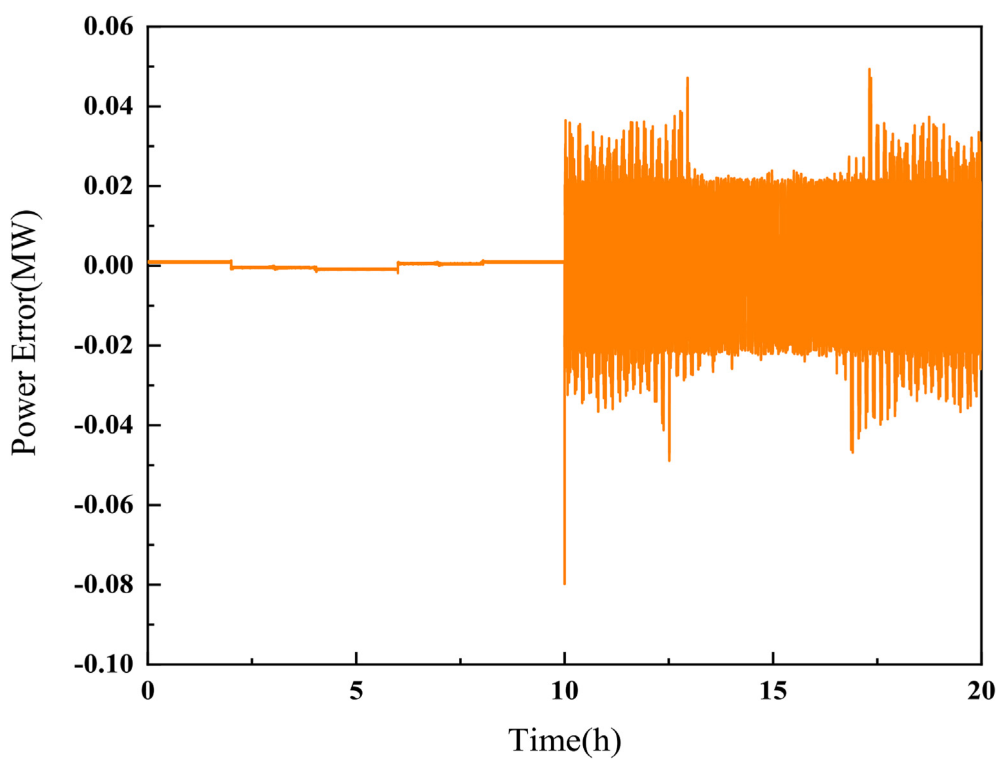

Fig. 4. Power tracking error under the action of the conventional SMC scheme.

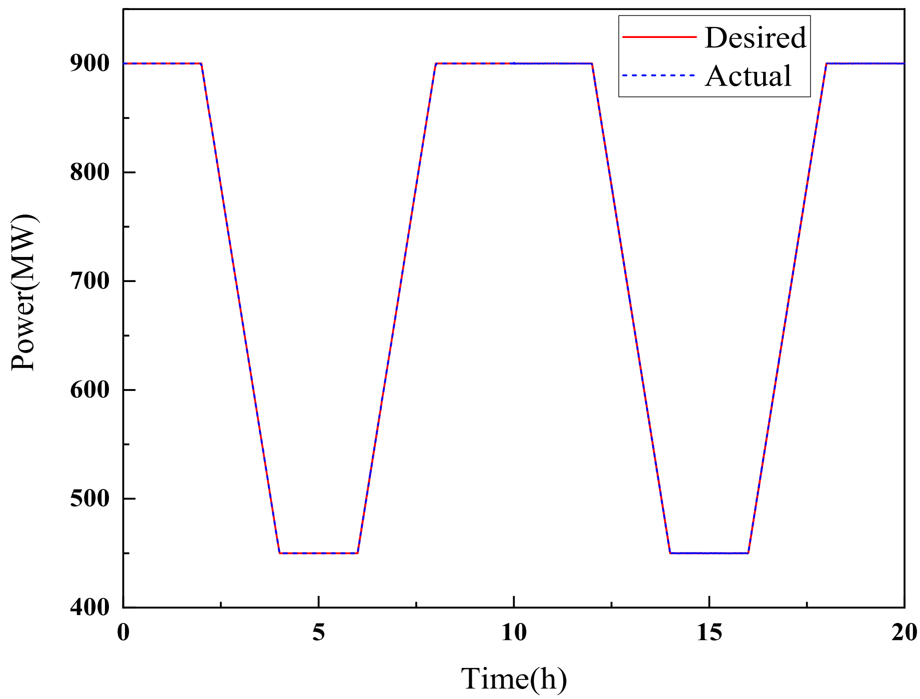

Fig. 5. Power tracking performance under the action of the PID controller.

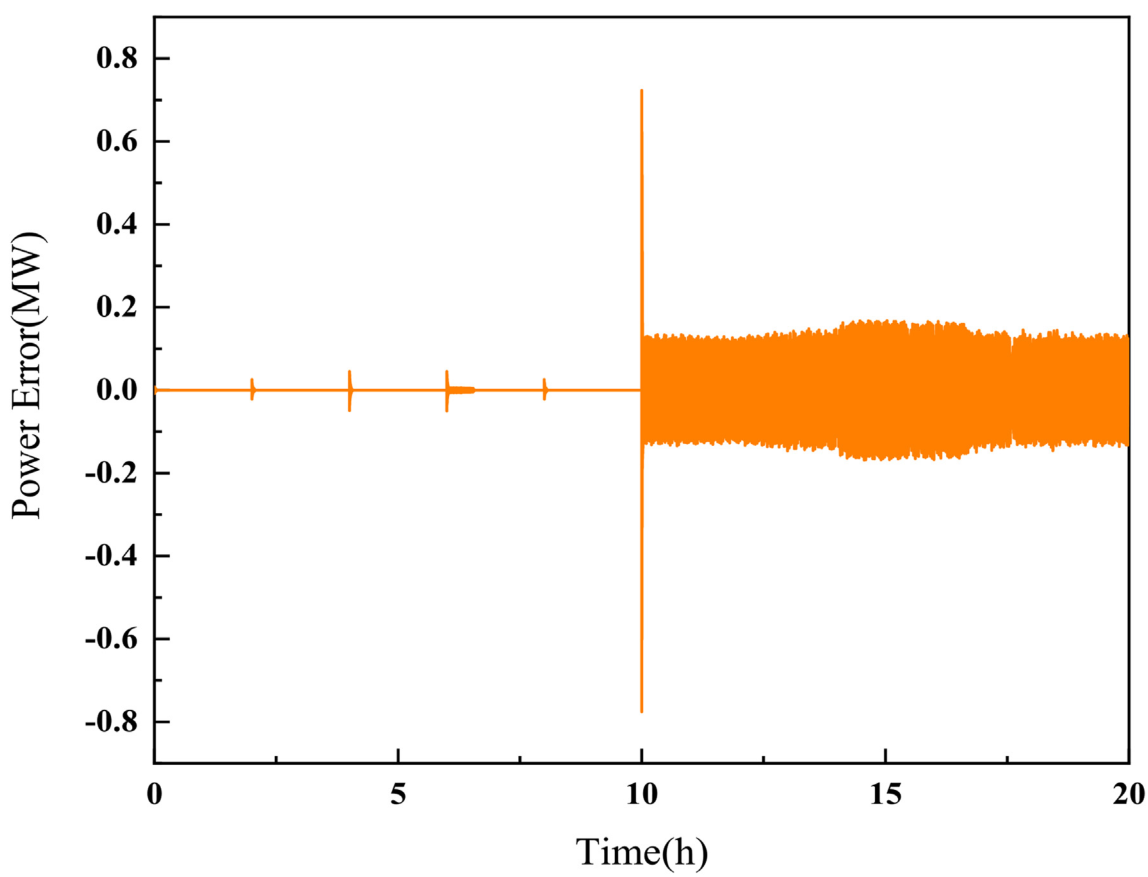

Fig. 6. Power tracking error under the action of the PID controller.

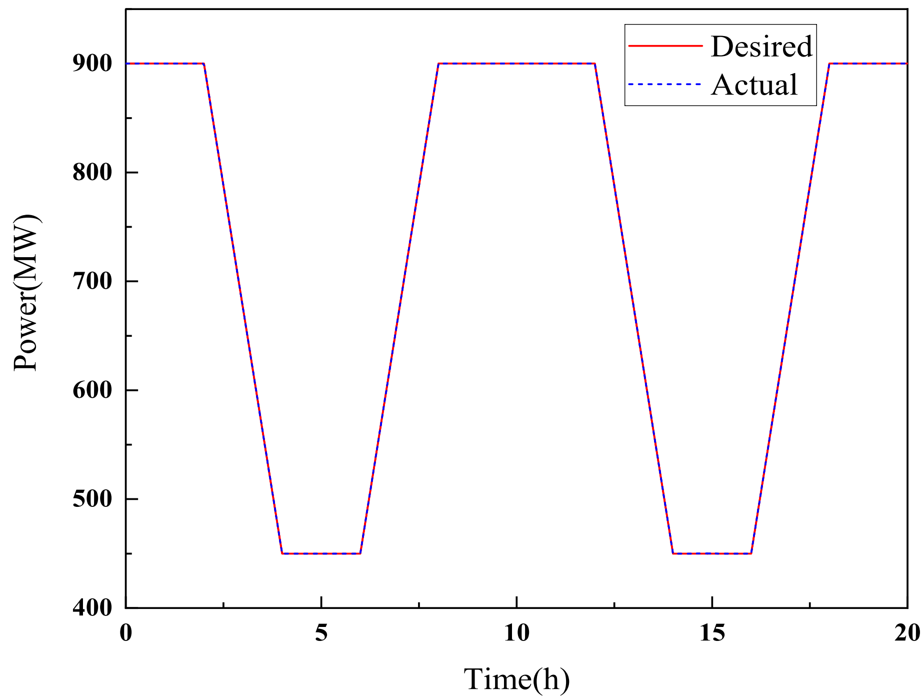

Fig. 7. Power tracking performance under the action of the conventional backstepping controller.

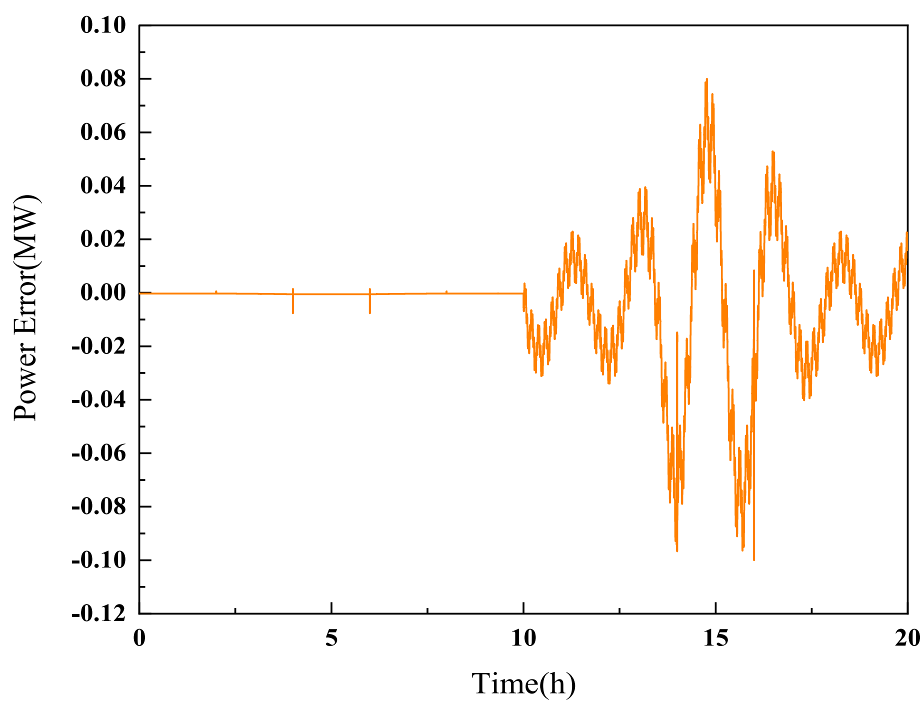

Fig. 8. Power tracking error under the action of the conventional backstepping controller.

$$\frac{dn_r}{dt}=\frac{n_r}{\Lambda}\left[-\beta+\rho_r+\alpha_f\left(T_f-T_{f0}\right)+\frac{\alpha_c}{2}(T_l-T_{l0})+\frac{\alpha_c}{2}(T_e-T_{e0})\right.$$
$$\left.\times\right]+\sum_{i=1}^{6}\frac{\beta_i}{\Lambda}c_{ri}+d_2 \tag{8}$$

where $d_2=d+(\Delta_\rho n_r)/\Lambda$ denote lumped disturbances including reactivity disturbances, model uncertainties, and external disturbances.

3. Disturbance observer design

In this section, a new sliding mode disturbance observer is designed to estimate the lumped disturbances d_2 in real time, and their estimation values are used to control system design subsequently. Before the disturbance observer design, the following

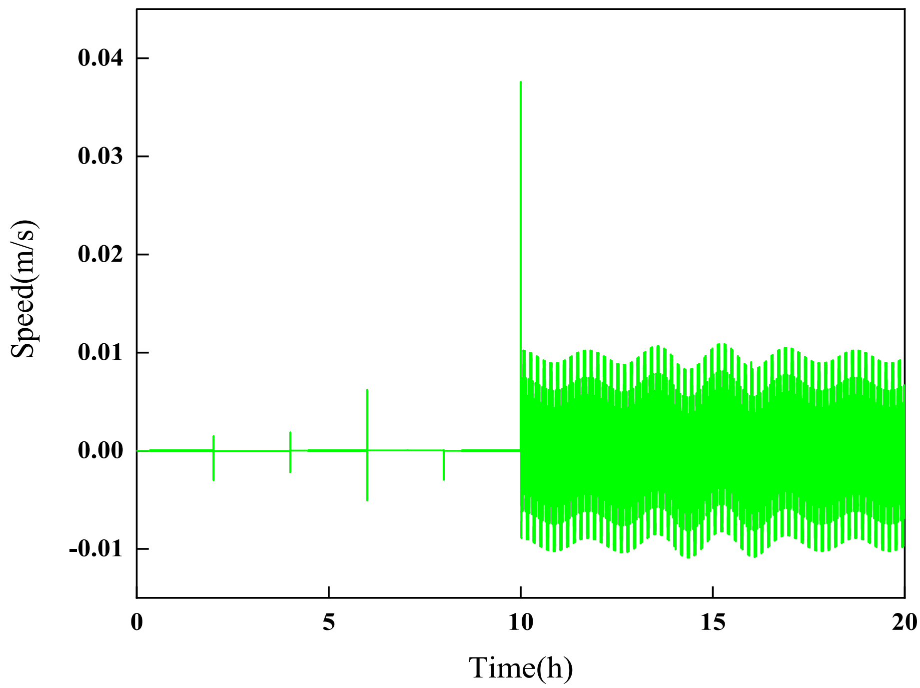

Fig. 9. The control rod speed for the DOB-ASMC scheme.

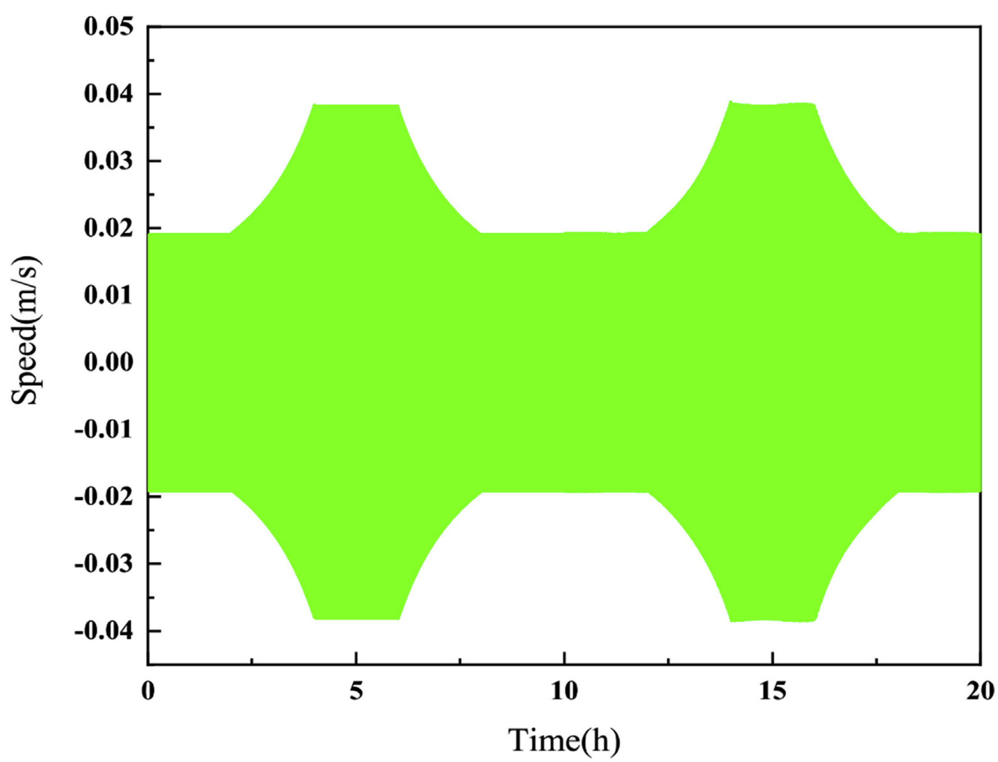

Fig. 10. The control rod speed for the conventional SMC scheme.

assumptions are introduced.

Assumption 1. The disturbances d_1 and d_2 are all bounded, i.e., $|d_1| \le D_1$ and $d_2 \le D_2$, where D_1 and D_2 are unknown upper bounds.

Assumption 2. The lumped disturbances d_2 vary very slowly, and the derivative of d_2 with respect to time is considered as $\dot{d}_2 = 0$

For the model of the PWR, if the relative density of ith delayed neutron precursor c_{ri} is regarded as virtual input, and the relative neutron density n_r and lumped disturbances d_2 are regarded as system outputs, the following linear state-space equation can be obtained as:

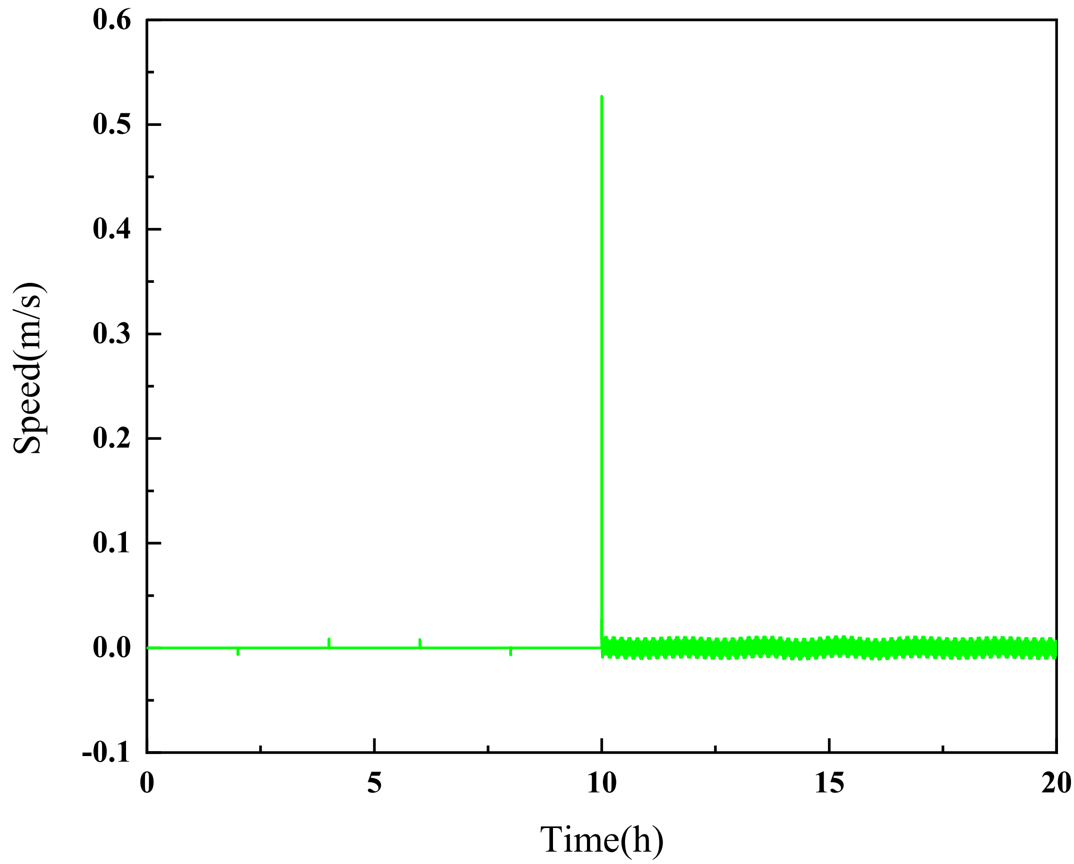

Fig. 11. The control rod speed for the PID controller.

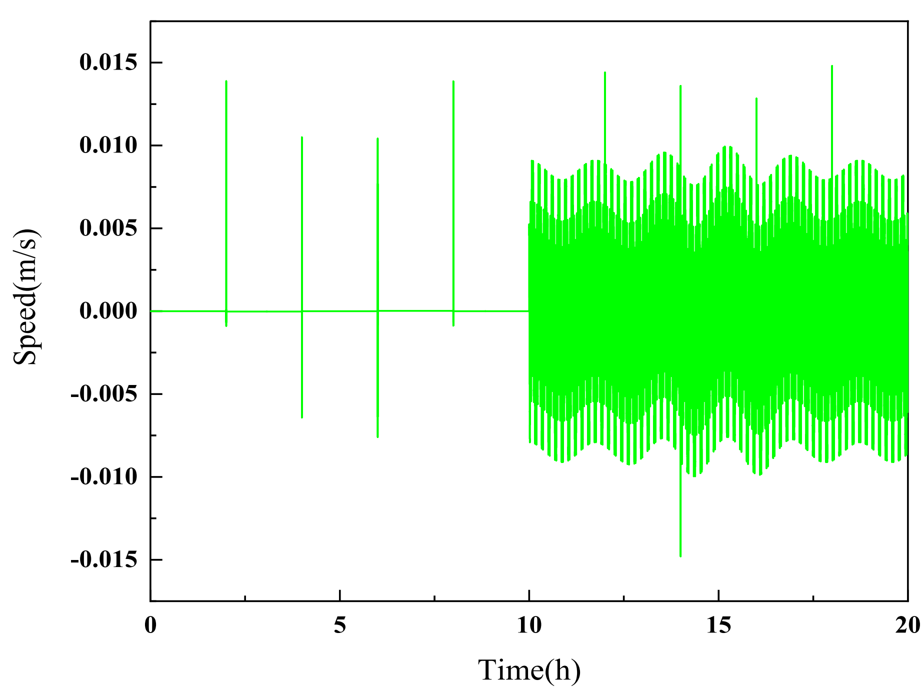

Fig. 12. The control rod speed for the conventional backstepping controller.

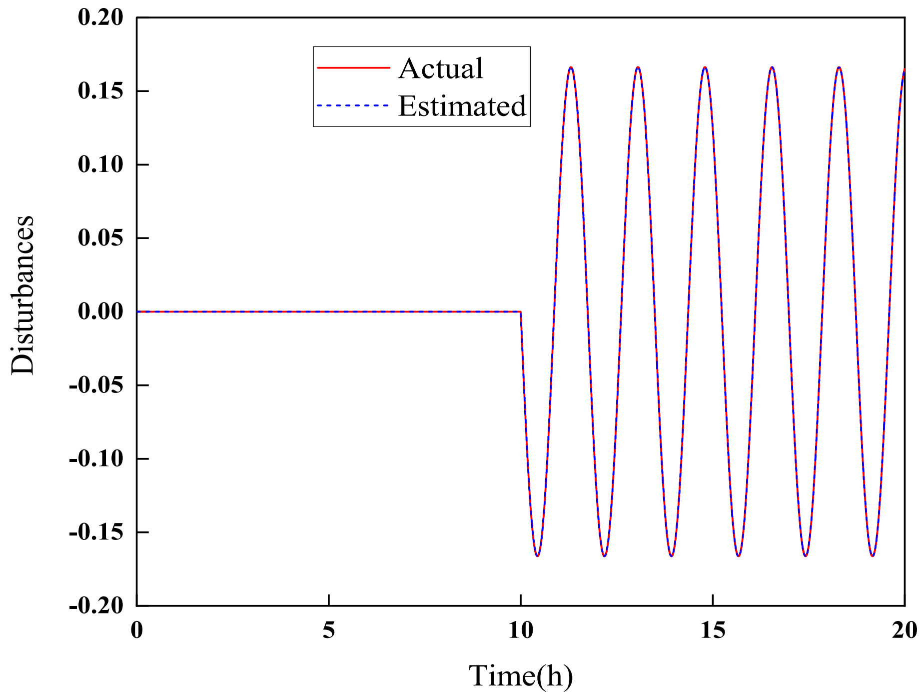

Fig. 13. Disturbances estimation by using the DOB.

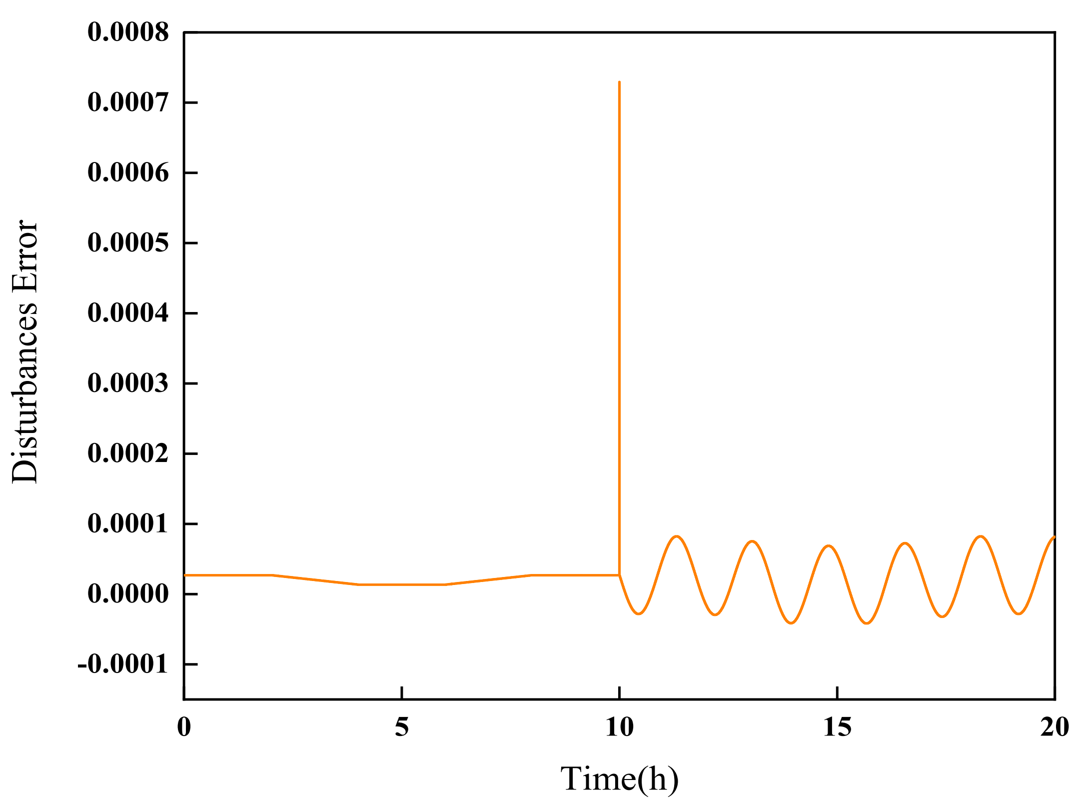

Fig. 14. Disturbances estimation error by using the DOB.

$$\begin{bmatrix}\dot{n}_r \\ \dot{d}_2\end{bmatrix} = \left[\frac{1}{\Lambda}\left[-\beta+\rho_r+\alpha_f\left(T_f-T_{f0}\right)+\frac{\alpha_c}{2}(T_l-T_{l0}) +\frac{\alpha_c}{2}(T_e-T_{e0})\right]100\right]\begin{bmatrix}n_r \\ d_2\end{bmatrix} + \sum_{i=1}^{6}\begin{bmatrix}\frac{\beta_i}{\Lambda} \\ 0\end{bmatrix}c_{ri} \tag{9}$$

From the linear state-space (9), the sliding mode disturbance observer is designed as

$$\begin{bmatrix}\dot{\hat{n}}_r \\ \dot{\hat{d}}_2\end{bmatrix} = \begin{bmatrix}\frac{1}{\Lambda}\left[-\beta+\rho_r+\alpha_f\left(T_f-T_{f0}\right)+\frac{\alpha_c}{2}(T_l-T_{l0})+\frac{\alpha_c}{2}(T_e-T_{e0})\right] & 1 \\ 0 & 0\end{bmatrix}\begin{bmatrix}\hat{n}_r \\ \hat{d}_2\end{bmatrix}+\sum_{i=1}^{6}\begin{bmatrix}\frac{\beta_i}{\Lambda} \\ 0\end{bmatrix}c_{ri}+\begin{bmatrix}1 \\ w\end{bmatrix}F(e_{n_r}) \tag{10}$$

where $\hat{n}_r$ and $\hat{d}_2$ denote the estimation values of n_r and d_2, respectively, w denotes the observer gain, $F(e_{n_r})$ denotes a sliding mode function, and need to be designed later. The observer errors are defined as

$$\begin{cases} e_{n_r} = n_r - \hat{n}_r \\ e_{d_2} = d_2 - \hat{d}_2 \end{cases} \tag{11}$$

Differentiating the observer errors (11) with respect to time, and combining equations (9) and (10) yields

$$\begin{cases} \dot{e}_{n_r} = \frac{e_{n_r}}{\Lambda}\left[-\beta+\rho_r+\alpha_f\left(T_f-T_{f0}\right)+\frac{\alpha_c}{2}(T_l-T_{l0})+\frac{\alpha_c}{2}(T_e-T_{e0})\right]+e_{d_2}-F(e_{n_r}) \\ \dot{e}_{d_2} = -wF(e_{n_r}) \end{cases} \tag{12}$$

Then, defining the following integral sliding mode surface as

$$s_{n_r} = e_{n_r} + k_1\int_0^t e_{n_r}(\tau)d_\tau \tag{13}$$

where k_1 is a positive constant to be determined later. In order to make the estimation values $\hat{n}_r$ and $\hat{d}_2$ converge to the actual values n_r and d_2 asymptotically, the sliding mode function $F(e_{n_r})$ is designed as

$$F(e_{n_r}) = e_{n_r}\left\{k_1+\frac{1}{\Lambda}\left[-\beta+\rho_r+\alpha_f\left(T_f-T_{f0}\right)+\frac{\alpha_c}{2}(T_l-T_{l0})+\frac{\alpha_c}{2}(T_e-T_{e0})\right]\right\} + k_{n_r}s_{n_r}+h_{n_r}\text{sat}(s_{n_r}) \tag{14}$$

where $h_{n_r}>0$ and $k_{n_r}>0$ denote switching gain and reaching gain, respectively. sat($\bullet$) denotes saturation function, and it is defined as

$$\text{sat}(s) = \begin{cases} 1 & \text{if } s>\Delta_s \\ \frac{s}{\Delta_s} & \text{if } |s|\le\Delta_s \\ -1 & \text{if } s<-\Delta_s \end{cases} \tag{15}$$

where $\Delta_s>0$ denotes the boundary layer thickness. Consider the following Lyapunov function candidate as:

$$V_1 = \frac{1}{2}s_{n_r}^2 \tag{16}$$

Differentiating (16) with respect to time along (13), and substituting (14) yields

$$\begin{aligned} \dot{V}_1 &= s_{n_r}\dot{s}_{n_r} \\ &= s_{n_r}\left\{\frac{e_{n_r}}{\Lambda}\left[-\beta+\rho_r+\alpha_f\left(T_f-T_{f0}\right)+\frac{\alpha_c}{2}(T_l-T_{l0}) +\frac{\alpha_c}{2}(T_e-T_{e0})\right] +e_{d_2}-F(e_{n_r})+k_1e_{n_r}\right\} \\ &= s_{n_r}\left[e_{d_2}-k_{n_r}s_{n_r}-h_{n_r}\text{sat}(s_{n_r})\right] \end{aligned} \tag{17}$$

In order to make $\dot{V}_1<0$, the following condition must be satisfied:

$$h_{n_r}+k_{n_r}\Delta_{s_r}>|e_{d_2}| \tag{18}$$

As a result, according to Lyapunov stability theory [26], it is obtained from (18) that the observer error dynamic moves toward from anywhere and reaches the sliding mode surface $s_{n_r}=0$ in finite time with suitable parameters h_{n_r}, k_{n_r}, and Δ_{s_r}. When the sliding mode surface $s_{n_r}=0$ is reached, we have

$$\begin{cases} s_{n_r} = \dot{s}_{n_r} = 0 \\ e_{n_r} = \dot{e}_{n_r} = 0 \end{cases} \tag{19}$$

Substituting (19) into (12) yields

$$\begin{cases} e_{d_2} = F(e_{n_r}) \\ \dot{e}_{d_2} = -wF(e_{n_r}) \end{cases} \tag{20}$$

Therefore, the observer error dynamic of the lumped disturbances with respect to time is obtained as

$$e_{d_2} = c_d e^{-wt} \tag{21}$$

where c_d is a constant. From (17), (18), and (21), it can be concluded that the observer error dynamics of the DOB are globally asymptotically stable. In addition, the convergence speed can be regulated by changing the value of the observer gain w.

4. Adaptive sliding mode control design

The aim of this paper is to design the power tracking controller for the PWR with lumped disturbances. This section presents the power tracking controller design using backstepping technique and integral sliding mode control approach as well as the disturbances estimation values $\widehat{d}_2$ from the DOB. Moreover, an adaptive law is introduced to estimate the input uncertainties d_1 online. At first, the power error is defined as

$$e_p = P - P_d \tag{22}$$

An integral sliding mode surface for power control is chosen as

$$s_p = e_p + k_2 \int_0^t e_p(\tau) d_\tau \tag{23}$$

where k_2 is a positive constant to be determined later. Differentiating (23) with respect to time, and substituting (7), (8), and (22) yields

$$\begin{aligned} \dot{s}_p &= \dot{e}_p + k_2 e_p \\ &= \dot{P} - \dot{P}_d + k_2 e_p \\ &= P_0 \left\{ \frac{n_r}{\Lambda} \left[-\beta + \rho_r + \alpha_f \left(T_f - T_{f0} \right) + \frac{\alpha_c}{2} (T_l - T_{l0}) + \frac{\alpha_c}{2} (T_e - T_{e0}) \right] \right. \\ &\quad \left. + \sum_{i=1}^{6} \frac{\beta_i}{\Lambda} c_{ri} + d_2 \right\} - \dot{P}_d + k_2 e_p \end{aligned} \tag{24}$$

According to backstepping technique [26,27], the reactivity due to the position movement of control rod ρ_r is regarded as virtual control input, and its desired value is designed as

$$\begin{aligned} \rho_{rd} &= \beta - \alpha_f \left(T_f - T_{f0} \right) - \frac{\alpha_c}{2} (T_l - T_{l0}) - \frac{\alpha_c}{2} (T_e - T_{e0}) \\ &+ \frac{\Lambda}{P_0 n_r} \left[-P_0 \sum_{i=1}^{6} \frac{\beta_i}{\Lambda} c_{ri} - P_0 \widehat{d}_2 + P_d - k_2 e_p - k_p s_p - h_p \mathrm{sat}(s_p) \right] \end{aligned} \tag{25}$$

where ρ_{rd} denotes the desired reactivity due to control rod position movement, $h_p > 0$ and $k_p > 0$ denote switching gain and reaching gain, respectively. The reactivity error is defined as

$$e_\rho = \rho_r - \rho_{rd} \tag{26}$$

Consider the following Lyapunov function candidate:

$$V_2 = \frac{1}{2} s_p^2 \tag{27}$$

Differentiating (27) with respect to time, and substituting (24), (25), and (26) yields

$$\begin{aligned} \dot{V}_2 &= s_p \dot{s}_p \\ &= s_p P_0 \left\{ \frac{n_r}{\Lambda} \left[-\beta + \rho_r + \alpha_f \left(T_f - T_{f0} \right) + \frac{\alpha_c}{2} (T_l - T_{l0}) \right. \right. \\ &\quad \left. \left. + \frac{\alpha_c}{2} (T_e - T_{e0}) \right] + \sum_{i=1}^{6} \frac{\beta_i}{\Lambda} c_{ri} + d_2 \right\} \\ &= s_p P_0 \left\{ \frac{n_r}{\Lambda} \left[-\beta + e_\rho + \rho_{rd} + \alpha_f \left(T_f - T_{f0} \right) + \frac{\alpha_c}{2} (T_l - T_{l0}) \right. \right. \\ &\quad \left. \left. + \frac{\alpha_c}{2} (T_e - T_{e0}) \right] + \sum_{i=1}^{6} \frac{\beta_i}{\Lambda} c_{ri} + d_2 \right\} \\ &= \frac{s_p P_0 n_r e_\rho}{\Lambda} + s_p P_0 e_{d_2} - k_p s_p^2 - h_p s_p \mathrm{sat}(s_p) \end{aligned} \tag{28}$$

The next step is to make ρ_r converge to ρ_{rd}, i.e., $\lim_{t \to +\infty} e_\rho \to 0$. To this end, the control law Z_r needs to be designed to guarantee the stability of the overall control system. Defining the following Lyapunov function candidate:

$$V_3 = V_2 + \frac{1}{2} e_\rho^2 \tag{29}$$

Differentiating (29) with respect to time, and substituting (4) and (28) yields

$$\begin{aligned} \dot{V}_3 &= \dot{V}_2 + e_\rho \dot{e}_\rho \\ &= s_p P_0 e_{d_2} - k_p s_p^2 - h_p s_p \mathrm{sat}(s_p) + e_\rho \left(\frac{s_p P_0 n_r}{\Lambda} + \dot{\rho}_r - \dot{\rho}_{rd} \right) \\ &= s_p P_0 e_{d_2} - k_p s_p^2 - h_p s_p \mathrm{sat}(s_p) + e_\rho \left(\frac{s_p P_0 n_r}{\Lambda} + G_r Z_r + d_1 - \dot{\rho}_{rd} \right) \end{aligned} \tag{30}$$

In order to make $\dot{V}_3 < 0$, the control law can be designed as

$$Z_r = \frac{-s_p P_0 n_r + \Lambda[\dot{\rho}_{rd} - d_1 - k_\rho e_\rho - h_\rho \mathrm{sat}(e_\rho)]}{\Lambda G_r} \tag{31}$$

where $h_\rho > 0$ and $k_\rho > 0$ denote switching gain and reaching gain, respectively. However, given that the input uncertainties d_1 is unknown and bounded, in this study, an adaptive mechanism is employed to approximate the input uncertainties d_1 online, and the adaptive law is designed as

$$\dot{\widehat{d}}_1 = \kappa e_\rho \tag{32}$$

where κ is a positive constant, and needs to be determined later. Besides, the approximation error is given as

$$e_{d_1} = d_1 - \widehat{d}_1 \tag{33}$$

To this end, the control law can be rewritten as

$$Z_r = \frac{-s_p P_0 n_r + \Lambda[\dot{\rho}_{rd} - \widehat{d}_1 - k_\rho e_\rho - h_\rho \mathrm{sat}(e_\rho)]}{\Lambda G_r} \tag{34}$$

Next, consider the following Lyapunov function candidate:

$$V_4 = V_3 + \frac{1}{2\kappa} e_{d_1}^2 \tag{35}$$

Differentiating (35) with respect to time, and substituting (30), (32), and (34) yields

$$\begin{aligned}\dot{V}_4 &= \dot{V}_3 - \frac{1}{\kappa} e_{d_1} \dot{\hat{d}}_1 \\ &= s_p P_0 e_{d_2} - k_p s_p^2 - h_p s_p \mathrm{sat}(s_p) + e_\rho \left(\frac{s_p P_0 n_r}{\Lambda} + G_r Z_r + d_1 - \dot{\rho}_{rd} \right) \\ &\quad - \frac{1}{\kappa} e_{d_1} \dot{\hat{d}}_1 \\ &= s_p P_0 e_{d_2} - k_p s_p^2 - h_p s_p \mathrm{sat}(s_p) - k_\rho e_\rho^2 - h_\rho e_\rho \mathrm{sat}(e_\rho) \\ &\quad + e_{d_1} \left(e_\rho - \frac{1}{\kappa} \dot{\hat{d}}_1 \right) \\ &= s_p P_0 e_{d_2} - k_p s_p^2 - h_p s_p \mathrm{sat}(s_p) - k_\rho e_\rho^2 - h_\rho e_\rho \mathrm{sat}(e_\rho)\end{aligned} \tag{36}$$

As a result, it can be followed from (36) that in order to make $\dot{V}_4 < 0$, the following condition should be satisfied:

$$h_p + k_p \Delta_{s_p} > |e_{d_2}| P_0 \tag{37}$$

where Δ_{s_p} denotes the boundary layer thickness of the sliding mode surface (23).

In summary, consider the nuclear reactor system in the presence of disturbances d_1 and d_2, and satisfying Assumptions 1 and 2, conditions (18) and (37), and adaptive law (32), under the action of control law (34), then the error vector $e = [e_p \; e_\rho \; e_{d_1} \; e_{d_2}]^T$ asymptotically converge to zero. As a result, the overall control system is globally asymptotically stable.

Remark 1. It is well known that chatting phenomenon in SMC is one of the greatest disadvantages, which may increase the energy consumption, stimulate system unmodeled dynamics, degrade control performance, and even cause unstable system. In this study, the conventional sign function of the SMC is replaced by saturation function to reduce the chatting phenomenon, which is called as boundary layer SMC [28].

5. Simulation results

Simulation studies and comparisons based on the PWR system are provided in this section to demonstrate the effectiveness of the DOB-based disturbances estimation and the DOB-ASMC scheme. It is well known that PID controller is popular owing to its better dynamic and static quantity, simple structure, and mature capability to tune parameters. Therefore, comparisons of power tracking performances are made between the proposed DOB-ASMC strategy, PID controller, conventional nonlinear SMC scheme [29], and conventional backstepping controller [26]. The change rule of the desired power is composed of two identical periods (per 10 h), i.e., $100\%P_0 \rightarrow 60\%P_0 \rightarrow 100\%P_0 \rightarrow 60\%P_0 \rightarrow 100\%P_0$. The first period is with the assumption that the nuclear reactor model is accurate without disturbances d_1 and d_2. The second period is with the assumption that the nuclear reactor model is uncertain and the disturbances d_1 and d_2 are added in the model. The detailed parameter values of the PWR model are listed in Table 1.

For the DOB-ASMC scheme, the parameter values are chosen as: $w = 200$, $k_1 = 100$, $k_2 = 10$, $k_{n_r} = 50$, $h_{n_r} = 50$, $k_p = 100$, $h_p = 100$, $k_\rho = 30$, $h_\rho = 20$, $\kappa = 2$, $\Delta_{s_{nr}} = 0.001$, $\Delta_{s_p} = 0.1$, and $\Delta_{s_\rho} = 0.01$.

In addition, the disturbances d_1 and d_2 are assumed as follows:

$$\begin{cases} d_1 = 0.005 \sin(0.01t - 1.8586) + 0.003\cos(0.05t - 1.4382) \\ d_2 = 0.1663 \cos\left(10^{-3}t - 0.1335\right) \end{cases} \tag{38}$$

The simulation results are presented in Fig. 1–14. Figs. 1–8 illustrate the power tracking performance and power error under the action of the DOB-ASMC scheme, conventional SMC scheme, PID controller, and conventional backstepping controller. From Figs. 1–8, it can be seen that all control approaches provide precise power tracking performance for the nominal PWR system before adding the disturbances d_1 and d_2. However, after adding the disturbances d_1 and d_2 in the second period, i.e., 10–20 h, it is clearly observed from Figs. 1–8 that the DOB-ASMC strategy features strong robustness with respect to disturbances and rejects disturbances d_1 and d_2 effectively, while the conventional SMC scheme and PID controller as well as conventional backstepping controller cannot deal with disturbances effectively, which lead to clearly non-zero fluctuating error. Figs. 9–12 plot the control rod speed under the action of the DOB-ASMC scheme, conventional SMC scheme, PID controller, and conventional backstepping controller. As observed in Fig. 11, extremely high control rod speed is produced by the PID controller when the disturbances d_1 and d_2 are added in the PWR system compared with the DOB-ASMC scheme and conventional SMC scheme as well as conventional backstepping controller. In practical engineering, such overhigh control rod speed can not be achieved due to the physical constraints.

Figs. 13–14 show the estimation performance of the designed DOB. From Figs. 13–14, it is demonstrated that the designed DOB is able to estimate the lumped disturbances d_2 accurately regardless of adding disturbances d_1 and d_2. In addition, transient peaking estimation error may occur at the moment of adding the disturbances d_1 and d_2, while the DOB swiftly estimates the disturbances d_2 with acceptable error.

From the above analysis of the simulation results, it is concluded that the overall DOB-ASMC strategy can provide more exact power tracking performance compared with conventional SMC scheme and PID controller as well as conventional backstepping controller together with accurate disturbances estimation by using the DOB in the presence of unknown lumped disturbances caused by input uncertainties, reactivity disturbances, model uncertainties, and external disturbances.

6. Conclusions

In this paper, power tracking problem of a PWR with lumped disturbances has been addressed by developing a DOB-ASMC strategy. Firstly, the mathematical model of the PWR system is established and then a new DOB is implemented to accurately achieve lumped disturbances estimation online. Based on the established mathematical model of the PWR and disturbances estimation from the DOB, an adaptive sliding mode controller is proposed combining backstepping technique with sliding mode control method to guarantee the globally asymptotic stability of the overall closed-loop power tracking system, which contributes to improving power tracking performance and enhancing the disturbances rejection ability for a PWR with lumped disturbances. In the end, the simulation results reveal that the proposed DOB-ASMC strategy can achieve higher power tracking performance, stronger robustness with respect to disturbances, and better disturbances rejection ability than the conventional SMC scheme and PID controller as well as conventional backstepping controller.

Acknowledgements

This study is supported by the Open Project Program of the State Key Laboratory of Nuclear Power Safety Monitoring Technology and Equipment of China (Grant No. K-A2019.426) and the Natural Science Foundation of Shanghai (Grant No. 17ZR1414200).

Appendix A. Supplementary data

Supplementary data related to this article can be found at https://doi.org/10.1016/j.net.2020.04.027.

References

[1] Cody Yuling Hsiao, Hsing Hung Chen, The contagious effects on economic development after resuming construction policy for nuclear power plants in coastal China, Energy 152 (2018) 291–302.
[2] M. Zarei, A multi-point kinetics based MIMO-PI control of power in PWR reactors, Nucl. Eng. Des. 328 (2018) 283–291.
[3] Seyed Mohammad Hossein Mousakazemi, Navid Ayoobian, Gholam Reza Ansarifar, Control of the reactor core power in PWR using optimized PID controller with the real-coded GA, Ann. Nucl. Energy 118 (2018) 107–121.
[4] Ramazan Coban, A fuzzy controller design for nuclear research reactors using the particle swarm optimization algorithm, Nucl. Eng. Des. 241 (5) (2011) 1899–1908.
[5] Saptarshi Das, Indranil Pan, Shantanu Das, Fractional order fuzzy control of nuclear reactor power with thermal-hydraulic effects in the presence of random network induced delay and sensor noise having long range dependence, Energy Convers. Manag. 68 (2013), 200–218.
[6] Jae Hwan Kim, Soon Ho Park, Man Gyun Na, Design of a model predictive load-following controller by discrete optimization of control rod speed for PWRs, Ann. Nucl. Energy 71 (2014) 343–351.
[7] Guoxu Wang, Jie Wu, Bifan Zeng, Zhibin Xu, Wanqiang Wu, Xiaoqian Ma, State-space model predictive control method for core power control in pressurized water reactor nuclear power stations, Nucl. Eng. Technol. 49 (2) (2016) 1–7.
[8] Yuyan Liu, Jizhen Liu, Shiliang Zhou, Linear active disturbance rejection control for pressurized water reactor power, Ann. Nucl. Energy 111 (22–30) (2018).
[9] Guoxu Wang, Jie Wu, Bifan Zeng, Zhibin Xu, Xiaoqian Ma, A nonlinear adaptive sliding mode control strategy for modular high-temperature gas-cooled reactors, Prog. Nucl. Energy 113 (2019) 53–61.
[10] Guoxu Wang, Jie Wu, Bifan Zeng, Zhibin Xu, Xiaoqian Ma, A chattering-free sliding mode control strategy for modular high-temperature gas-cooled reactors, Ann. Nucl. Energy 133 (2019) 688–695.
[11] Nafiseh Zare Davijani, Gholamreza Jahanfarnia, Amir Esmaeili Abharian, Nonlinear fractional sliding mode controller based on reduced order FNPK model for output power control of nuclear research reactors, IEEE Trans. Nucl. Sci. 64 (1) (2016) 713–723.
[12] G. Datatreya Reddy, Youngjin Park, Bijnan Bandyopadhyay, A.P. Tiwari, Discrete-time output feedback sliding mode control for spatial control of a large phwr, Automatica 45 (9) (2009) 2159–2163.
[13] Zhe Dong, Adaptive proportional-differential power-level control for pressurized water reactors, IEEE Trans. Nucl. Sci. 61 (2) (2014) 912–920.
[14] G.R. Ansarifar, et al., Adaptive robust control for axial offset in the PWR nuclear reactors based on the multipoint reactor model during load-following operation, Ann. Nucl. Energy 103 (2017) 251–264.
[15] Inayet Ozge Aksu, Ramazan Coban, Sliding mode PI control with backstepping approach for MIMO nonlinear cross-coupled tank systems, Int. J. Robust Nonlinear Control 29 (6) (2019) 1854–1871.
[16] G.R. Ansarifar, Control of the nuclear steam generators using adaptive dynamic sliding mode method based on the nonlinear model, Ann. Nucl. Energy 88 (2016) 280–300.
[17] Zhengyu Huang, Robert M. Edwards, Kwang Y. Lee, Fuzzy-adapted recursive sliding-mode controller design for a nuclear power plant control, IEEE Trans. Nucl. Sci. 51 (1) (2004) 256–266.
[18] Mou Chen, Yu Jing, Disturbance observer-based adaptive sliding mode control for near-space vehicles, Nonlinear Dynam. 82 (4) (2015) 1671–1682.
[19] Cunjia Liu, Wen-Hua Chen, John Andrews, Tracking control of small-scale helicopters using explicit nonlinear MPC augmented with disturbance observers, Contr. Eng. Pract. 20 (3) (2012) 258–268.
[20] Zi-Jiang Yang, Youichirou Fukushima, Qin Pan, Decentralized adaptive robust control of robot manipulators using disturbance observers, IEEE Trans. Contr. Syst. Technol. 20 (5) (2011) 1357–1365.
[21] Haofeng Li, Wenzhen Chen, Lei Luo, Qian Zhu, A new integral method for solving the point reactor neutron kinetics equations, Ann. Nucl. Energy 36 (4) (2009) 427–432.
[22] Dale B. Cherchas, Samuel S. Ng, Optimum control of neutron flux during nuclear station load following, Automatica 14 (6) (1978) 533–546.
[23] Wenfeng Liu, Zhengpei Luo, Li Fu, Yaqi Wang, The three-dimensional power distribution control in load following of the heating reactor, Ann. Nucl. Energy 28 (8) (2001) 741–754.
[24] R. Coban, Computational intelligence-based trajectory scheduling for control of nuclear research reactors, Prog. Nucl. Energy 52 (4) (2010) 415–424.
[25] Zhe Dong, Power-level control for mhtgrs with time-delay in helium temperature measurement, IEEE Trans. Nucl. Sci. 61 (3) (2014) 1349–1359.
[26] Isidori Alberto, Nonlinear Control Systems, Springer Science & Business Media, 2013.
[27] Ramazan Coban, Adaptive backstepping sliding mode control with tuning functions for nonlinear uncertain systems, Int. J. Syst. Sci. 50 (8) (2019) 1517–1529.
[28] Pushkin Kachroo, Masayoshi Tomizuka, Chattering reduction and error convergence in the sliding-mode control of a class of nonlinear systems, IEEE Trans. Automat. Contr. 41 (7) (1996) 1063–1068.
[29] Hua Jing, An Li-Xia, Yi-Min Li, Bionic fuzzy sliding mode control and robustness analysis, Appl. Math. Model. 39 (15) (2015) 4482–4493.